DC TRANSFORMERS

A transformer is an indispensable part of most dc–dc power electronic converters. Its purpose is to provide galvanic isolation between windings, to provide single or multiple output signals, and to match the load characteristics to the input supply characteristics. Magnetic and piezoelectric isolation are the most popular forms of galvanic isolation. Magnetic isolation devices have kVA ratings that typically decrease with increasing frequency. At 1 kHz it is not uncommon to see 100 kVA designs. At 1.0 MHz it is uncommon to see ratings beyond 1 kVA. Piezoelectric isolation devices can be designed with maximum ratings on the order of 10 VA. Their operating frequency can range anywhere from 8 kHz to several MHz. The size of the device decreases with increasing frequencies. The design of a dc–dc converter requires an understanding of power conversion topologies, magnetic circuit or piezoelectric circuit modeling, dc motor drive, and control system theory (1–3).

The input dc is typically obtained by electronically converting the utility's nearly constant frequency input ac voltage (50 Hz or 60 Hz) to a dc voltage. Variable-frequency ac sources such as windmills, gas turbines, or diesel generators can also be considered. Alternatively the dc may be generated directly by photovoltaic cells, battery cells, fuel cells, or magnetohydrodynamic (MHD) methods (4).

Improvements in the semiconductor technology and the development of new circuit topologies and control techniques have made it possible to increase the switching frequency of the power electronic converters. This has resulted in the reduction of the reactive component size and an increase in the power density of a given converter unit. The upper bound on switching frequency is ultimately limited by the losses in the components, particularly magnetic components, and by concerns over electromagnetically generated interference.

Definition of a Dc Transformer

The combination of a transformer, an input dc source, and a power electronic converter that converts the incoming dc source to an isolated single output dc source or multiple isolated output dc sources is henceforth referred to as a dc transformer. A dc transformer can be realized in the following two ways: an input dc signal is converted to an ac signal, the ac signal is transformed, and finally the output signal or signals are rectified [Fig. 1(a)]; or an input dc signal is transformed directly to one or more dc signals [Fig. 1(b)].

Magnetic Isolation

Various magnetic and winding structures for transformers have been developed to prevent loss and electomagnetic interference, for instance, planar sandwich transformers, meander transformers, multielement transformers, pot core transformers, and toroidal transformers to name only a few (5–8). It becomes increasingly difficult to predict the performance of a transformer as the frequency of operation is increased. This stems from the fact that an ideal transformer model becomes less and less applicable. Therefore, a more accurate model that can be used to characterize the performance of the trans-

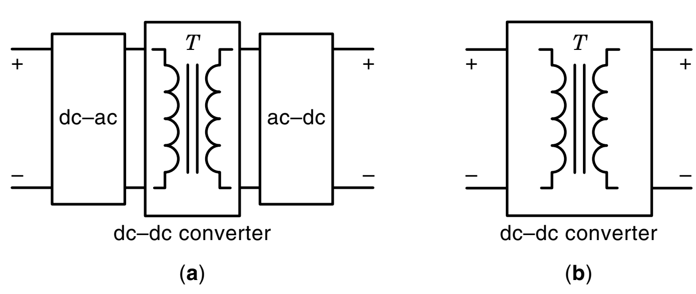

Figure 1. Dc transformer realizations: (a) indirect-driven transformer, (b) direct-driven transformer.

former must be considered and must take into account the following data: magnetic core loss (hysteresis and eddy current); winding loss; leakage flux; inter- and intra-winding displacement currents.

Modeling data such as core loss are determined empirically, whereas eddy current winding loss, leakage flux, and displacement currents are estimated using computer-aided design (CAD) or computer-aided engineering electromagnetic (CAE EM) software tools.

Alternative Methods of Isolation

NEC in Japan has developed a piezoelectric transformer that shows promising results at high operating frequencies and that can be used for low-power applications such as portable electronic equipment (2). This type of transformer, when operated at high frequencies, has the following advantages: the energy density is higher than in a magnetic transformer, the internal power losses (dielectric loss and mechanical loss) are low and do not increase as the operating frequency increases; the skin and proximity effects are almost negligible; the transformer is small in size and has a thin planar structure and a high power density (e.g., a transformer having a 2 mm thickness can handle power levels up to 10 W); no electromagnetic interference is generated by the transformer.

Other isolation techniques have been developed recently, such as optical and electromagnetic wave (microwave) isolation, but the power efficiency and capacity of both of these isolation techniques are limited (9).

DC TRANSFORMER OPERATING PRINCIPLES

The transformation process can be accomplished either directly or indirectly. The indirect method uses a high-frequency ac intermediate link, and as a result no dc magnetic flux exists within the transformer. In contrast, the transformer flux for a directly transformed system has a dc component. A representative diagram illustrating these differences is shown in Fig. 2(a) and 2(b). For both cases, the average voltage across the transformer winding over one switching period, or alternatively the volt–second integral over one period, must be equal to zero. Otherwise the transformer will saturate and will not function as designed.

Magnetic Transformer

Impressed Ac Flux (Bidirectional Core Excitation). A bipolar generated current waveform at the primary terminals of the transformer will generate an ac flux swing and can be accomplished in one of the following two ways: by capacitively coupling a dc voltage with superimposed nonsinusoidal ac waveform to the primary winding in order to remove the dc voltage component, and by impressing an arbitrary ac voltage with harmonic content across the primary winding of the transformer.

A simplified representation of these two excitation schemes is shown in Fig. 2(c) and 2(d). The secondary coils in both cases are connected to a rectifier circuit. The choice of one rectifier over another will depend on application considerations. A controlled rectifier can also be considered; however, its use requires an appropriate application environment.

Impressed Dc Flux (Unidirectional Core Excitation). An impressed unipolar current waveform at the primary terminals of the transformer will result in a dc flux swing in the transformer core. There are a number of ways in which this flux swing can be generated from a circuit standpoint. This is described in more detail in a later section.

Low-Frequency Equivalent Circuit. The equivalent circuit for a low-frequency core type transformer is shown in Fig. 3(a). R_1 and R_2 represent the primary and secondary winding resistances respectively; L_1 and L_2 represent the primary and secondary leakage inductances respectively; L_m represents the magnetizing inductance referred to the primary side; R_c represents the equivalent resistance corresponding to core losses; N_1/N_2 represents the ideal transformer primary-to-secondary turns ratio. L_1 and L_2 must be vanishingly small and L_m must be large in order for the transformer to be considered

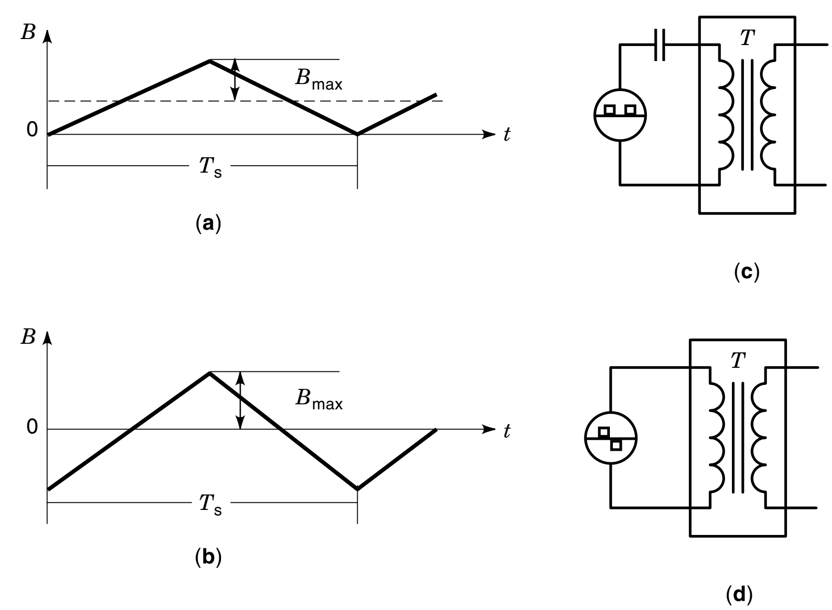

Figure 2. Transformer flux and circuit operation for achieving linear operation: (a) dc flux, (b) ac flux, (c) capacitor-coupled transformer, (d) ac voltage-coupled transformer.

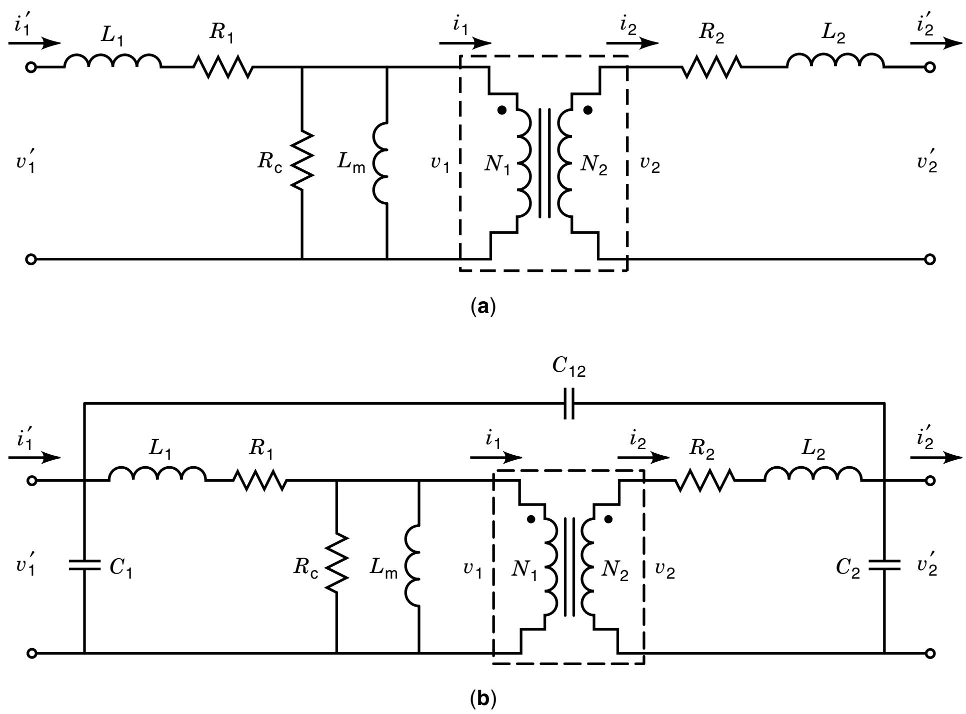

Figure 3. Transformer lumped parameter equivalent circuit model: (a) low-frequency transformer model, (b) high-frequency transformer model.

as nearly ideal. Leakage inductance is a function of both core geometry and winding configuration. Solenoidal coil constructions are known to have a smaller leakage reactance than planar constructions.

High-Frequency Equivalent Circuits. It becomes difficult to ignore the effects of the leakage inductances and the intra- and interwinding capacitances at operating frequencies above 100 kHz or if the turns ratio is very large. At moderate frequencies it is reasonable to lump together the effects of stray capacitances and leakage inductances. At very high frequencies, the windings are represented as distributed circuit elements rather than as lumped circuit elements. Lumped parameter models can be used to analyze the harmonic impedances, whereas distributed circuit models can be used to analyze the harmonic impedances and the transient voltage distribution in a transformer winding (10).

Lumped Parameter Equivalent Circuit Model. Figure 3(b) shows a lumped parameter equivalent circuit representation of a transformer. It is not uncommon to have leakage inductances in the nanohenry to microhenry range and stray capacitances on the order of picofarads. These parasitic elements generate undesirable overvoltage transients in low-frequency applications and unwanted resonant circuit behavior at higher operating frequencies. Resonances can be exploited in a constructive way if the parasitic effects are taken into account in the design process. In the high-frequency transformer equivalent circuit, C_1 and C_2 represent the distributed primary and secondary shunt capacitance respectively (intrawinding capacitances), L_1 and L_2 represent the primary and secondary leakage inductance respectively, R_1 and R_2 represent the primary and secondary winding resistances respectively, C_{12} represents the primary-to-secondary capacitance (interwinding capacitance), R_c represents the equivalent resistance corresponding to core losses, L_m represents the equivalent magnetizing inductance referred to the primary side, and N_1/N_2 represents the ideal transformer primary-to-secondary turns ratio.

Piezoelectric Transformer

The basic structure of the piezoelectric transformer (PT) consists of two piezoelectric crystals separated by a thin insulating nonpiezoelectric material as shown in Fig. 4(a). A PT can operate in a longitudinal or a thickness extensional vibration mode (11,12). The transformer losses for the latter mode are substantially less than for the former. Therefore a design that uses the thickness extensional vibration mode is more advantageous.

The plane of polarization for the two crystals, as represented by the arrows in Fig. 4(a), is different (13). A PT converts an alternating electric field excitation within the first piezoelectric crystal to a mechanical vibration. The vibration is transmitted from the first piezoelectric crystal through the insulating layer to the second piezoelectric crystal. The vibrations within the second crystal generate an electric field variation in the second crystal. The time-varying electric field within the first and the second crystal represents a time-varying voltage across each crystal's output terminals. The transformer turns ratio N is equal to the thickness ratio of the input to the output crystal. The turns ratio can be altered by changing the relative thickness of the input and output layers.

The PT is designed to operate at high frequencies. Overall losses can be minimized if the transformer is connected to a low-switching-loss converter such as zero-voltage switching converter. The highest output efficiency is achieved if the output includes a shunt inductor. The inductor provides a path for the output dc current and also eliminates the output reactive power at a specific frequency.

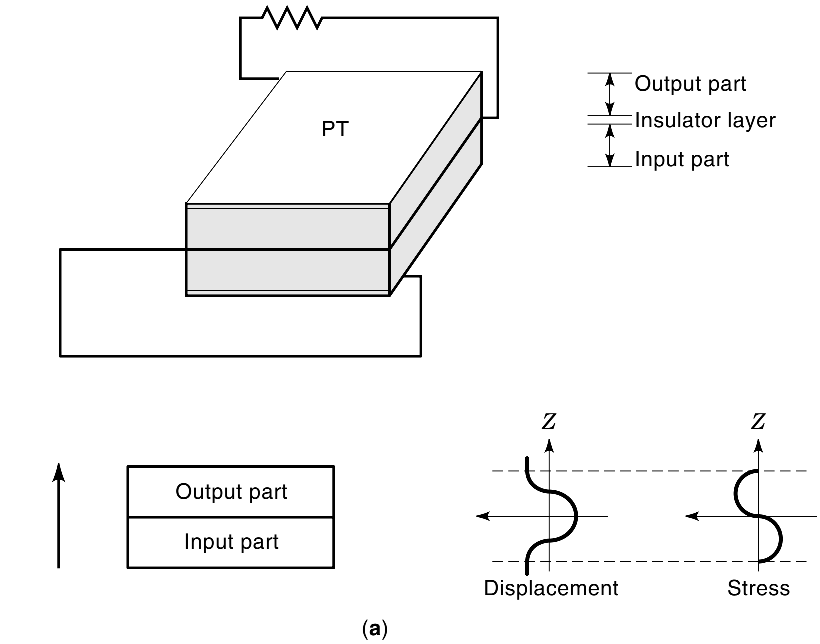

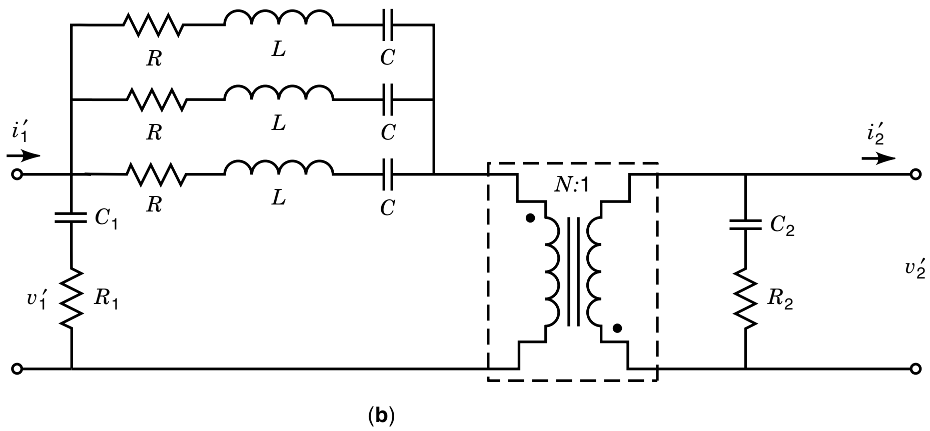

Figure 4. Piezoelectric transformer: (a) basic structure, (b) distributed constant high-frequency equivalent circuit.

High-Frequency Equivalent Circuit

A distributed-constant high-frequency equivalent circuit for a PT is shown in Fig. 4(b) (14). The resistors in the two capacitive shunt branches represent the internal losses. Three series resonant branches in parallel are incorporated into the model to represent the fundamental and two overtones of the piezoelectric crystal structure. The output–input transfer function for the PT circuit represents that of a bandpass filter.

DC TRANSFORMER APPLICATIONS AND PERFORMANCE

Dc transformers are used in a number of applications, such as telecommunication, computer, and electronic equipment; power factor correction circuits; distributed dc power transmission, and motion control.

Dc Transformer Classification

Dc transformers can be designed to operate in one of the following four modes: current source input and current source output; current source input and voltage source output; voltage source input and current source output; voltage source input and voltage source output.

Output voltage control necessitates the use of a capacitor across the output terminals, whereas output current control necessitates the use of an inductance in series with the output path. A similar statement holds for the case of an input voltage source and an input current source, except that the terminals become the input terminals.

Switching Matrices

The primary winding of the transformer is connected to a switching matrix in a specific way. The secondary winding of the transformer is connected to a diode rectifier. The switch matrix structures that can be used to build a dc transformer are shown in Fig. 5 and share common diode rectifier configurations.

The switching matrix structures are typically classified in terms of their power flow properties (unipolar or bipolar output current, and unipolar or bipolar output voltage) and

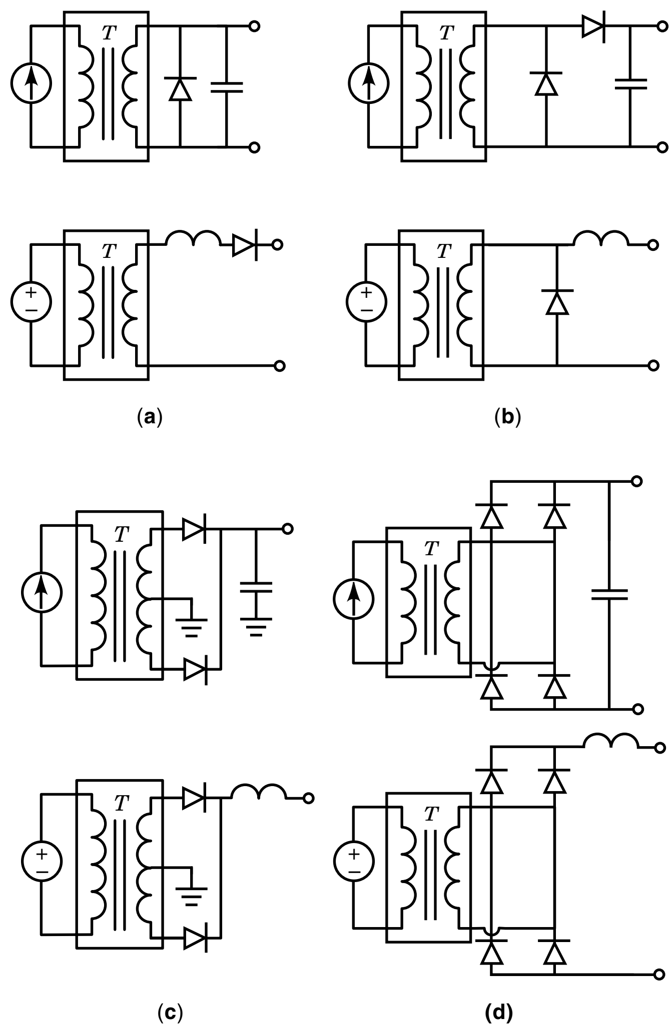

Figure 5. Dc transformer with various rectifying circuits: (a) half-wave, (b) class D, (c) class D center-tapped, (d) class D bridge.

whether they are fed by a current source or a voltage source. Low-power current source converters have the disadvantage of having a low power-to-weight ratio compared to voltage source converters. Therefore these converters are rarely used at low power levels, but are sometimes used in higher-power applications. The voltage-input, voltage-output implementation will be discussed in more detail, since it is the most common.

MOSFETs (metal oxide field effect transistors) are used as switches at high frequencies. IGBTs (insulated gate bipolar transistors) are used at moderate frequencies and moderate power levels. GTOs (gate-assisted turnoff thyristors) are used at low switching frequencies and high power levels. SCRs (silicon-controlled rectifiers) are used at extremely high power levels and require special commutation circuits to turn the switches off.

Ultrafast-recovery *pin* diodes are used if the peak inverse voltage requirements are high. Schottky diodes are used if the peak inverse voltage requirement is below 200 V. Synchronous rectifiers (i.e., MOSFETs gated to act as diodes) are an attractive alternative to a schottky rectifier if the combined gate drive, switching and conduction losses are less than the schottky conduction losses. This condition occurs with low voltage output designs (< 5 V) and MOSFET switching frequencies less than 500 kHz.

Leakage Inductance Application Criteria

Dc transformers are designed either to exploit the nonideal characteristics of the transformer or to minimize the nonideal characteristics. Designs of the former type exploit the leakage inductance and the magnetizing inductance as part of a resonant circuit. There are a number of resonant modes that can be utilized, depending on the application objectives. In all cases, goal is to minimize the switching losses in the converter switches (15). The design of a dc transformer with a specific leakage inductance and magnetizing inductance is not considered, because it requires an application-specific design process linked to the choice of additional reactive elements. Some general issues related to the design process are described in the following subsections.

The other design approach is to minimize the leakage inductance. Even a small amount of leakage inductance poses problems, since the energy stored in the leakage inductance must be extracted when the source or load is disconnected from the transformer during a converter switching transition. Failure to extract the stored energy results in destructive voltages and high-frequency transients during the switching transitions. Various lossy and lossless energy recovery circuits have been designed to address these problems (16,17). The ultimate benefits of a low-leakage-inductance design are a low stored energy and thus a smaller energy recovery circuit and a more efficient converter. Ultimately there exists a lower bound on the amount of leakage inductance. Therefore, beyond a certain operating frequency the efficiency of the power conversion process will decrease.

Dc Transformers with and without Intermediate Energy Storage

The magnetizing inductance can be used as an active storage element, as is the case with a flyback converter. Alternatively, its effects can play no direct role, in which case the transformer transfers energy directly from the input to the output without an intermediate energy storage phase. This is the case, e.g., for the forward converter.

It is common to introduce an air gap in the core if the transformer is to also act as an energy storage device. The air gap allows the designer to choose the value of the magnetizing inductance.

Dc Transformers Designed with a Low Leakage Inductance

A wide variety of dc transformer circuit topologies with a low leakage inductance have been documented in the literature. Only the most commonly used circuit topologies are discussed briefly. Other circuit topologies and details can be found in other references (18,19).

The core of the dc transformer used in low-leakage designs is exposed to either a unidirectional or a bidirectional excitation source. Unidirectional core excitation occurs when the first quadrant of the B–H loop is traversed. This condition exists for the flyback converter, flyback resonant converter, forward converter, and forward resonant converter. Bidirectional core excitation occurs when quadrants 1 and 3 of the B–H loop are traversed alternatively. This condition exists

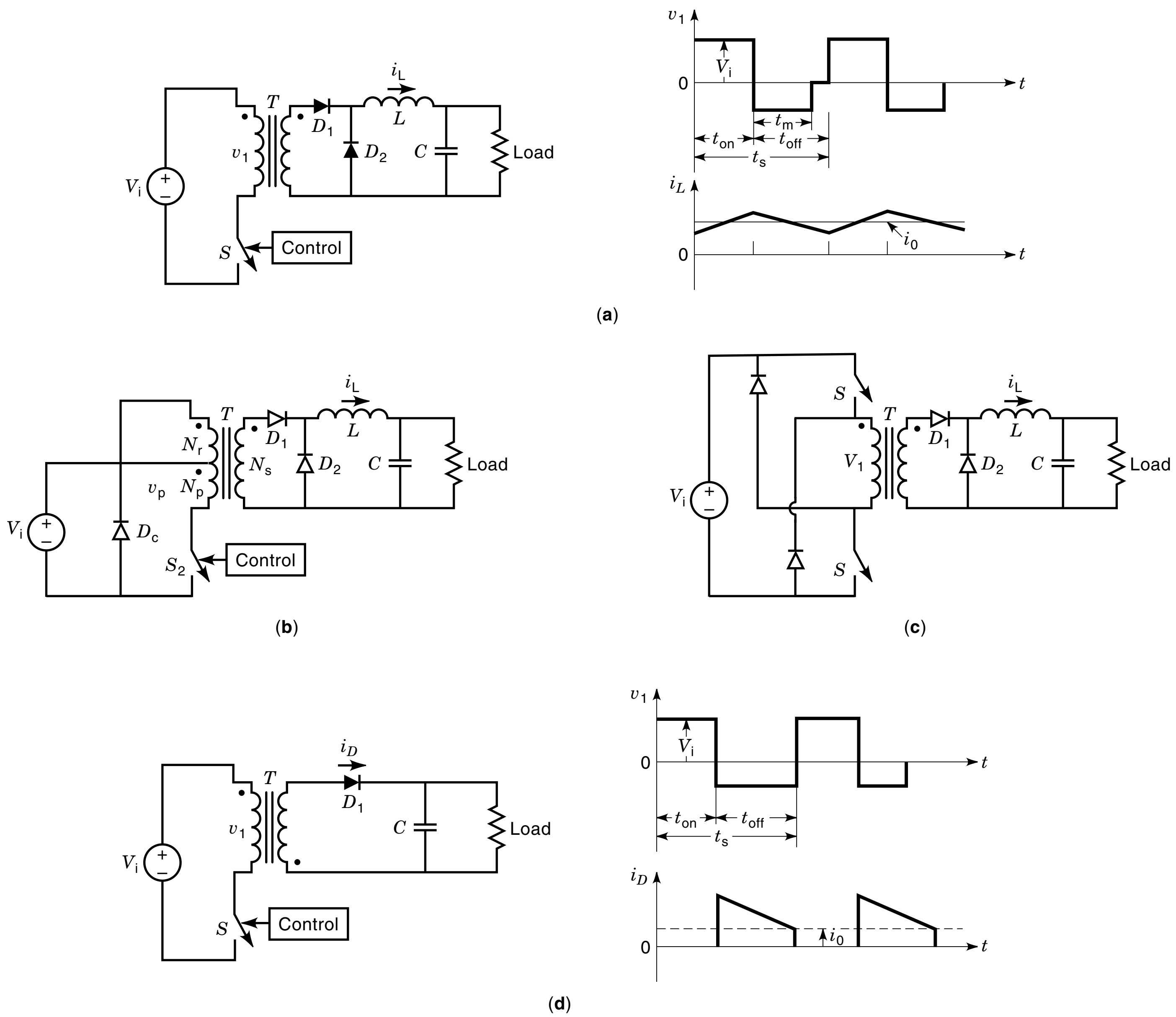

Figure 6. Converters with an unidirectional core excitation: (a) forward converter and its waveform, (b) center-tapped transformer winding, (c) two-transistor forward converter, (d) flyback converter and its waveform.

for the push–pull converter, the half-bridge converter, and the full-bridge converter.

Converters with a Unidirectional Core Excitation

Forward Converter. An idealized forward converter and the steady-state operating waveforms for the input voltage and output current are shown in Fig. 6(a). The forward converter topology is the most widely used switching converter topology for output powers under 500 W and when the dc input voltage lies in the range of 60 V to 200 V. This converter resembles the buck converter in that the switch in the basic switching converter is replaced by the combination of transformer, switch, and rectifier.

In a practical forward converter, the transformer magnetizing current must be reset to zero after each cycle so as to maintain the transformer in the unsaturated state. There are two ways in which this can be accomplished:

Using a Center-Tapped Transformer Primary Winding. The source is connected to one end of the half winding, and the switch is connected to the center tap as shown in Fig. 6(b). The other half of the winding, sometimes referred to as the tertiary winding, is connected across the input supply through a series diode. The purpose of the tertiary winding is to provide a path for reducing the magnetizing current to zero after the main switch is turned off and before another switching cycle begins.

Using a Two-Transistor Forward Converter. The two-transistor forward converter eliminates the tertiary winding but uses a transistor and diode to effectively clamp the peak transistor voltage to the line as shown in Fig. 6(c). The voltage ratings of the switches in this implementation are half of that in a single-switch implementation. More significantly, magnetizing current can flow through the diodes when the switches are off, thus eliminating the need for the tertiary winding and energy recovery snubbers (20,21).

The transfer function of the forward converter can be expressed as follows:

$$\frac{V_o}{V_i} = D\frac{N_2}{N_1} \tag{1}$$

where V_o/V_i is the input-to-output voltage ratio, N_1/N_2 is the turns ratio, and D is the duty cycle. D should be kept smaller than 0.5 so as to avoid transformer saturation.

Flyback Converter. Figure 6(d) shows the circuit schematic and steady-state operating waveforms for a flyback converter operating in the continuous mode (i.e., the magnetizing current is always greater than zero). The converter can be designed to operate in the discontinuous or the continuous mode. The discontinuous-mode flyback converter is sometimes used because it provides better output voltage regulation in response to sudden changes in load current or input voltage than the continuous-mode flyback converter. On the other hand, the discontinuous-mode flyback converter has a higher peak current for a given output average current.

The flyback converter is widely used for high-voltage applications and at low power levels. Flyback converters with multiple output voltages have a better output voltage tracking capability than most other switching converter topologies, since they do not require an output inductor. Energy is stored in the magnetizing inductor during the time period t_{on} and transferred to the load during the period t_{off}. A double-switch implementation is also possible, in which case the voltage rating of the switches is one-half that of the single-switch version. Also, an energy recovery snubber is not required to remove the energy stored in the primary winding leakage inductance.

The transfer function for the flyback converter can be expressed as follows:

$$\frac{V_o}{V_i} = \frac{N_2}{N_1}\left(\frac{D}{1-D}\right) \tag{2}$$

where V_o/V_i is the input-to-output voltage ratio, N_1/N_2 is the turns ratio, and D is the duty cycle. The flyback converter can have an output voltage that is higher or lower than the input voltage. The turns ratio N_1/N_2 of transformer is usually selected to provide a 50% duty cycle for a nominal output and input dc voltage. This operating duty cycle allows for the largest full scale swing in the duty cycle, either up or down, to allow for input voltage fluctuations.

Converters with a Bidirectional Core Excitation

Push–Pull Converter. Figure 7(a) shows the basic circuit schematic and steady-state operating waveforms for a push–pull converter. The push–pull converter is derived from two forward converters working in antiphase and has the advantage over a single-ended converter that the voltage across the transformer and hence the peak switch voltage is limited to twice the input voltage. This is due to the symmetrical center-tapped transformer, which has an equal number of turns in the primary windings.

The transfer function for the push–pull converter can be expressed as follows:

$$\frac{V_o}{V_i} = 2D\frac{N_2}{N_1} \tag{3}$$

where V_o/V_i is the input-to-output voltage ratio, N_1/N_2 is the turns ratio, and D is the duty cycle. D should be kept smaller than 0.5 so as to avoid simultaneous conduction of the two semiconductor switches. Also, current-mode control is used to prevent the switch currents from becoming unequal. Otherwise a dc current is forced into the transformer primary winding and as a result the transformer saturates.

Half-Bridge Converter. Figure 7(b) shows the circuit schematic and steady-state operating waveforms for a half-bridge switching converter. The half-bridge converter has a higher parts count than its single-ended counterparts and is used primarily in off-line switching converters and for higher-power applications. Its switches are not subjected to twice the input supply voltage as in the forward and push–pull switching converters. Two switches alternately connect one end of the transformer to $V_i/2$ and $-V_i/2$. The other end of the transformer is connected to the common terminal of the two identical filter capacitors C_1 and C_2. Ac transformer flux excursion is guaranteed, since one terminal of the transformer primary always sees an unbypassed capacitor in its path. Any unbalance in the device voltages or gating patterns results in an unequal voltage distribution across capacitors C_1 and C_2.

The half-bridge converter does not require any specific energy recovery circuit for the leakage reactance, because the energy stored in the leakage inductance is transferred back to the dc bus through the antiparallel diodes. In addition, the ac square-wave primary voltage produces a full-wave square waveform on all secondaries, similar to what is observed in the push–pull topology.

The transfer function for the half-bridge switching converter can be expressed as follows:

$$\frac{V_o}{V_i} = D\frac{N_2}{N_1} \tag{4}$$

where V_o/V_i is the input to output voltage ratio, N_1/N_2 is the turns ratio, and D is the duty cycle. Transformer saturation is avoided by preventing D from exceeding 0.5.

Full-Bridge Converter. Figure 7(c) shows the circuit schematic and steady-state operating waveforms for a full-bridge converter. The major advantage of a full-bridge circuit over the half-bridge circuit is the higher output voltage rating for a given switch voltage rating ($+V_{dc}$ and $-V_{dc}$ compared to $+V_{dc}/2$ and $-V_{dc}/2$). Thus, for transistors having the same peak current and voltage ratings, the full bridge is able to deliver twice the output power of the half bridge but requires twice as many transistors. This converter is generally used if the power rating of a half-bridge implementation is insufficient or if a greater degree of control over the output voltage

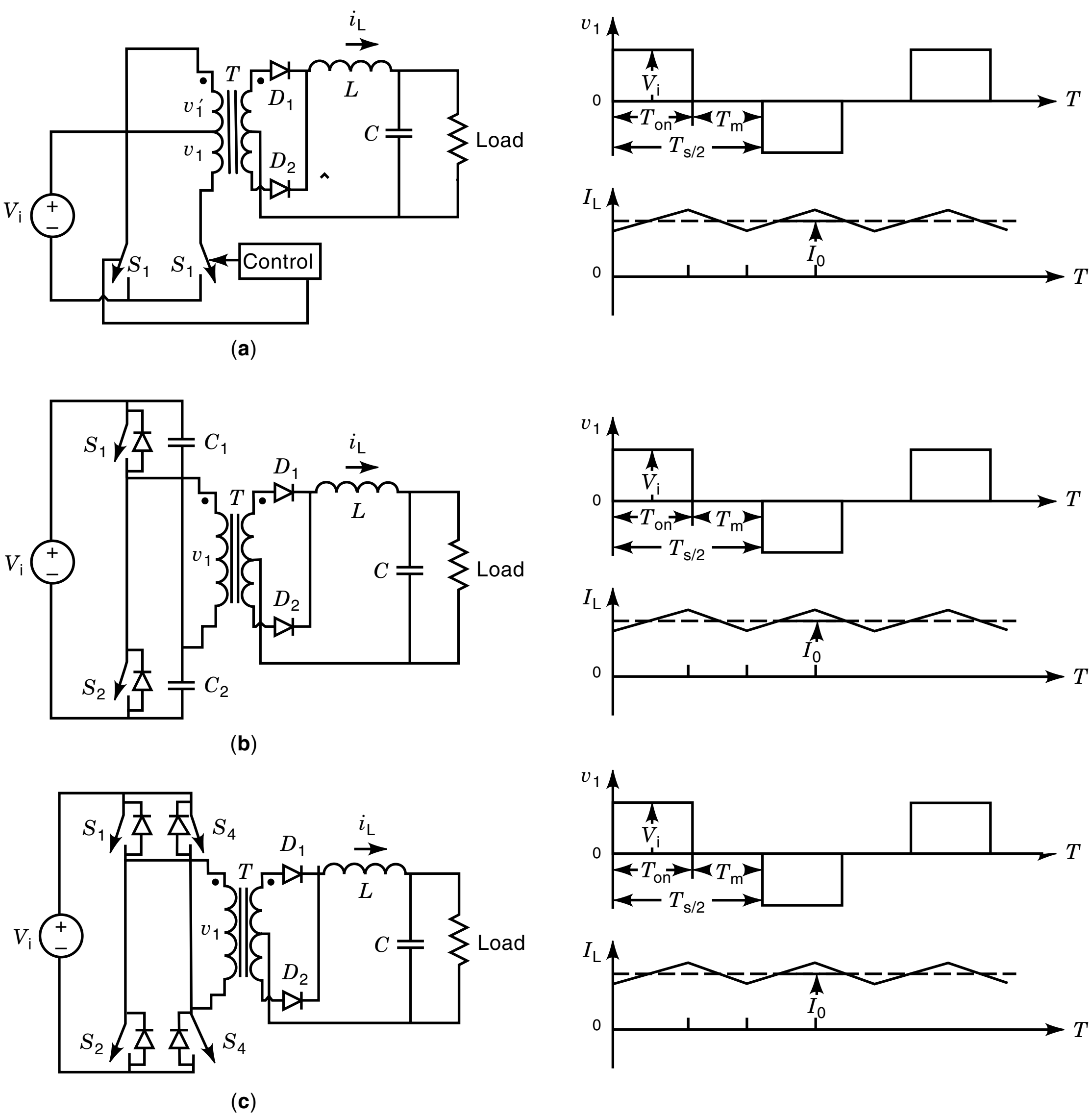

Figure 7. Converters with a directional core excitation: (a) push–pull switching converter and its waveform, (b) half-bridge switching converter and its waveform, (c) full-bridge switching converter and its waveform.

harmonic content is required (i.e., the voltage applied to the transformer terminals can be either V_{dc}, $-V_{dc}$, or 0).

Device voltage or gating signal unbalance will subject the transformer to a dc voltage and will result in transformer saturation. This can be avoided by:

Placing an ac Coupling Capacitor in Series with the Transformer. The capacitor value should be chosen so that it is not so large as to be ineffective under transient conditions and no so small as to cause a large ac voltage drop across it under steady-state operating conditions.

Implementing Current-Mode Control of the Converter. Current-mode control ensures that the primary winding current has a minimal dc component.

Introducing an Air Gap in the Transformer. The air gap allows a larger dc bias current to flow in the primary winding without forcing the core into saturation. The air gap decreases the magnetizing inductance and increases the no-load current.

Using a Flux Detector and Feedback. Magnetic flux is measured directly using a hall effect sensor or probe. The voltage detected across the sensor acts as a feedback signal and can be used to eliminate a dc flux offset in the core.

The transfer function of the full-bridge switching converter is expressed as follows:

$$\frac{V_o}{V_i} = 2D\frac{N_2}{N_1} \tag{5}$$

where V_o/V_i is the input to output voltage ratio, N_1/N_2 is the turns ratio, and D is the duty cycle.

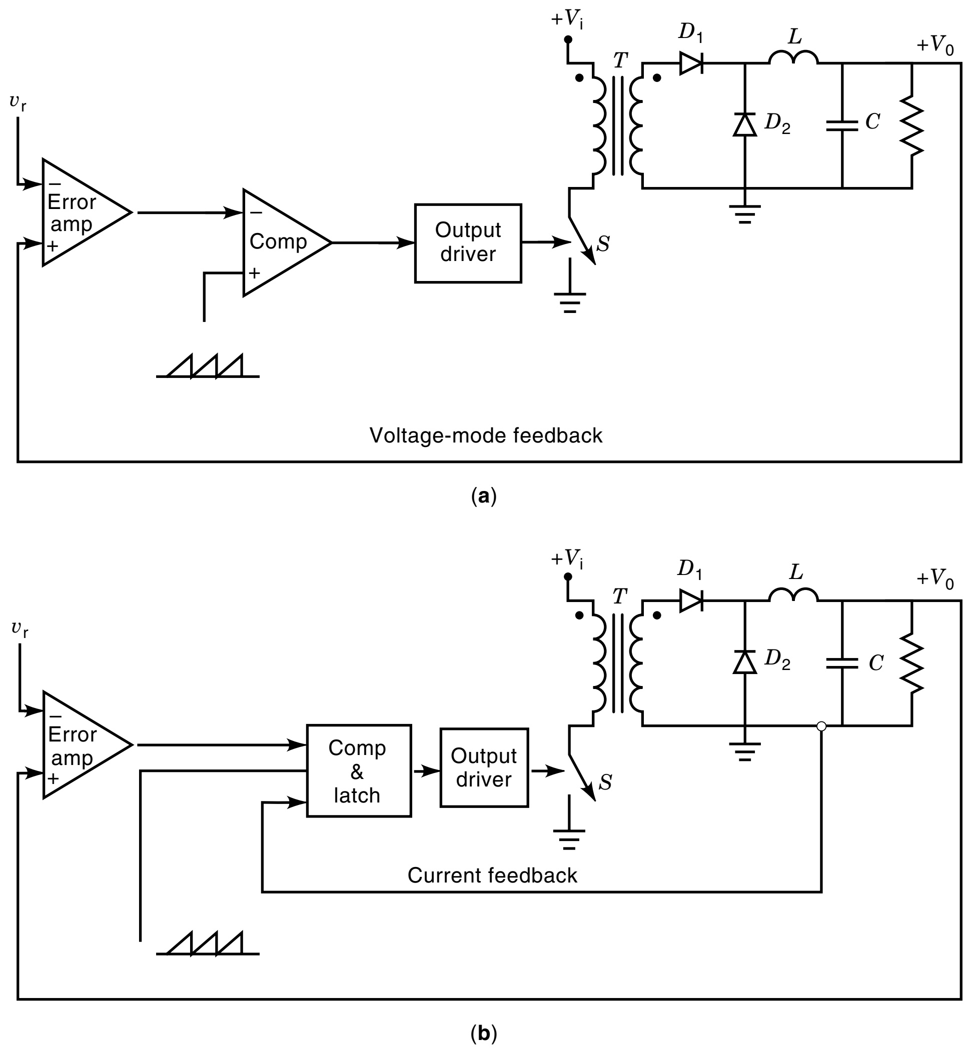

Figure 8. Voltage-mode versus current-mode control of dc–dc converters: (a) voltage mode, (b) current mode.

Gating and Control

Gating Strategies. Switching converters are classified as being either self-oscillating or driven. In the driven switching converter topologies, the output voltages are controlled by using a constant frequency PWM (pulse width modulation) controller, a hysteresis controller, or a controller with constant switch on-time or off-time. The main disadvantages of a driven system, especially at lower power levels, are the lower overall efficiency due to the losses in the gate driver circuit, mismatched output transistor characteristics, and saturation losses in the gate transformers.

The use of a particular gating strategy will be determined by application need. Control strategies other than fixed-switching-frequency PWM generate a continuous frequency spectrum rather than a discrete spectrum. Spectra consisting of discrete frequencies are easier to filter than spectra that have a nondiscrete frequency distribution or whose distribution varies with time. The filtering and gating strategy must be considered jointly in order to find a solution that addresses the regulations on conducted and radiated electromagnetic interference.

Control System Design. The design of a controller typically requires information on how the converter is to respond to dc input voltage changes, output load changes, and signal or sensor noise. The nature of these disturbances is of either a small-signal or a large-signal nature. Designs are normally made on the basis of a small-signal representation of the converter system. Regulators are then designed to meet performance specifications, after which the full circuit implementation is tested under large-signal disturbance conditions. Further refinements to the controller design may then be made on the basis of the observations.

The design of a controller involves the small-signal modeling of the power circuit, the modeling of the modulator, the selection of a control law, and the selection of a compensation circuit. The small-signal model is obtained by implementing a state-space-averaged model of the PWM circuit. The resultant model is then converted into a small-signal model about an operating point (22).

The following two methods are used to control the output voltage of a switching dc–dc power converter: voltage-mode control, in which the duty cycle of the converter is proportional to the error differential between the actual and ideal output voltages; and current-mode control, in which the duty cycle is proportional to the error differential between the nominal output voltage and an attenuated version of an appropriate controlling current combined with a compensating ramp. The controlling current can be either the switch current or the inductor current in a nonisolated topology, or the transformer primary current in an isolated topology (15).

Voltage-mode control responds only to changes in the output voltage. This means that in order for the converter to respond to changes in load current or input line voltage, it must wait for a corresponding change in load voltage (load regulation). This delay affects the regulation characteristics of the converter in that it is typically one or more switching cycles. Depending upon the load or line perturbation, there will be a corresponding output voltage perturbation, which can lead to a ripple instability problem for a number of duty cycles. A typical voltage-mode PWM control circuit is shown in Fig. 8(a).

Current-mode control creates a two-control-loop structure, consisting of current control via an inner control loop and voltage control via an outer control loop. The result is that changes in not only load voltage but also load curernt can be responded to on a pulse-by-pulse switching basis. A typical current-mode PWM control circuit is shown in Fig. 8(b). Details regarding current-injection mode control have been discussed by a number of authors (23,24).

DC TRANSFORMER MODELING

Magnetic Materials

Magnetic materials are characterized by their *M–H* curve. The initial slope is determined from the following relationship that exists between the magnetization *M* and the magnetic field intensity *H*:

$$H = \frac{B}{\mu_o} - M \tag{6}$$

where μ_o and B are the permeability of free space and the magnetic flux density respectively. Higher initial slopes indicate that the lines of flux will generally stay within the core material and thus leakage fluxes can be kept to a minimum. This is important if one is concerned about designing a near-ideal transformer. For a given application environment, a smaller core size can be selected if a material of higher saturation flux density is used.

Normally one measures the following relationship that exists between B and H where μ_r is the relative permeability:

$$H = \frac{B}{\mu_o \mu_r} \tag{7}$$

Typical *B–H* curves for a ferromagnetic material can be found from any textbook on magnetics. The area enclosed by the *B–H* curve is affected by the magnitude and frequency spectrum of the excitation waveform. Data provided by manufacturers usually refer to sinusoidal current excitation. The loop area represents the loss per unit volume per cycle due to hysteresis if the tests are carried out at a low enough frequency. This loss contributes to heating of the core and is generated because domain walls are unable to align themselves instantaneously with the externally applied magnetic field $\boldsymbol{H}$. It is desirable to select a loop area that is as small as possible.

Material Requirements for a Transformer. The fundamental rule for designing a transformer is to find a material with the highest relative permeability, the largest saturation flux density, the lowest core loss, and the lowest remanent flux density. The use of a material with low remanent flux density such as a powder core avoids the need for a transformer reset circuit. A high permeability is a necessary but not a sufficient condition for realizing an ideal transformer (i.e., one with low leakage inductance and high magnetizing inductance). Core geometry, winding layout, and winding shape are also important, especially at high frequencies and if the transformer has a high volt–ampere rating.

Material Requirements for a Linear Core. Many dc–dc converters contain reactive storage elements such as an inductor. Inductors should be designed with materials that exhibit low eddy current and hysteresis losses, that have a high saturation flux density, and whose permeability and shape can be designed to suit. This latter requirement is not usually met; therefore the designer must introduce an air gap. The introduction of a number of small air gaps rather than a large single air gap is usually advised. This action minimizes the effects of fringing fluxes, which generate proximity effect eddy current losses in the windings, especially at high frequencies.

The most common materials used for transformers in dc–dc converters are listed below and can be found in Ref. 18:

- *Silicon-laminated steels:* Frequency range <1 kHz; saturation flux density B_m = 2.0 T (20 kG); initial permeability <1,500
- *Ferrite (MnZn):* Frequency range 10 kHz to 2 MHz; B_m = 0.3 T to 0.5 T (3 kG to 5 kG); initial permeability <15,000
- *Ferrite (NiZn):* Frequency range 200 kHz to 100 MHz; B_m = 0.3 T to 0.5 T (3 kG to 5 kG); initial permeability <1500
- *Powder iron:* Frequency range 100 kHz to 100 MHz; B_m = 1.0 T (10 kG); initial permeability <100
- *Amorphous material:* For iron-based materials, frequency range 1 kHz to 100 kHz; B_m = 1.5 T to 1.6 T (15 kG to 16 kG); initial permeability <20,000; for cobolt-based materials, frequency <1 MHz; B_m = 0.5 T to 0.7 T (5 kG to 7 kG)
- *Nanocrystalline material:* Frequency <300 kHz; B_m = 1.2 T (12 kG); initial permeability <10,000

Magnetic Core and Winding Structures

Magnetic Core Structures. Various types of magnetic cores are commercially available. These core structures have the following advantages and disadvantages:

Pot core: Materials: Ferrite. High operating frequency, shielded winding, low EMI/RFI, inherent air gap, low heat transfer ability, and high core cost.

EE cores: Materials: Ferrite. Medium operating frequency, low core cost, low manufacturing cost, inherent air gap, no shielded winding.

Toroid core: Materials: Powdered iron, ferrite iron, amorphous magnetic material, and carbonyl iron. High operating frequency, low EMI/RFI, low core cost, no physi-

Table 1. Commonly Used Numerical Techniques and Their Computational Abilities[a]

Numerical Methods	Memory	CPU Time	Versatility	Preprocessing
Finite difference method	L	L	M	S
Finite element method	L	M/L	H	M
Boundary element method	S/M	S/M	M	S

[a]L = large, M = medium, S = small, and H = high.

cal air gap, high manufacturing cost, and no shielded winding.

Planar cores: Materials: Ferrite. High operating frequency, higher efficiency at higher frequencies, large surface area for cooling, inherent air gap, low core cost, low manufacturing cost, and low efficiency at lower frequencies (solenoidal construction is better at lower frequencies).

Winding Configurations. Transformer windings are normally made from copper because of its high conductivity. Skin and proximity effects cannot be ignored at high operating frequencies; therefore the winding structures have to be designed to minimize the eddy current losses. The advantages and disadvantages of the various winding configurations for high-frequency applications are as follows:

Sandwich coil: High operating frequency (<1 MHz), high proximity effect, low winding loss, low core cost, low- to medium-power application, low manufacturing cost, low winding inductance.

Toroidal coil: High operating frequency (<1 MHz), medium winding loss, medium- to high-power application, high manufacturing cost.

Planar spiral coil: High operating frequency (>10 MHz), low winding loss, low-power application, low winding inductance, low to medium manufacturing cost.

Planar meander coils: High operating frequency (>10 MHz), low winding loss, low- to medium-power applications, low winding inductance, medium manufacturing cost. The meander coil has a lower inductance per unit area but a better EMI performance.

U-shaped coil: High operating frequency (>10 MHz, broadband application), low winding loss, low- to medium-power applications, low winding inductance, medium manufacturing cost.

Numerical Techniques for Transformer Modeling

Electromagnetic Field Problems in Transformers. Many practical electromagnetic field problems in transformer design are extremely difficult or impossible to solve using analytic or simple circuit models. Analytic methods involve the solution of a system of mathematical equations that are functions of the desired variables.

Transformer problems can be formulated as magnetostatic problems at low frequencies. Eddy currents must be included at higher frequencies where the skin depth is no longer greater than the maximum dimension of the object under investigation. Displacement currents must be allowed for at even higher frequencies where the wavelength is of the same order or smaller than the largest dimension in a direction perpendicular to the magnetic field.

High-frequency problems can be solved using numerical techniques. Most of the CAD/CAE commercial software packages can operate on a PC MS-DOS, Windows, or Unix platform and can be used to design linear transformers and inductors. Software packages such as ANSOFT/EMAS, ANSOFT, VECTOR FIELDS, ANSYS, FLUX2D, INTEGRATED/OERSTED, INFOLYTICA, and AMPERES can also be used to solve two- or three-dimensional problems (25). Some of these packages can solve nonlinear electromagnetic, electromagnetic field distribution, eddy-current, and coupled problems.

Numerical Modeling Techniques and CAD/CAE. Numerical methods such as the method of moments, the finite difference method, and the finite element method were firmly established during the 1970s, and were used widely to solve electromagnetic field problems in the 1980s (26,27). Another method, called the boundary element method, was introduced into electrical engineering at the end of the 1970s and was used extensively in the 1980s (28–30). The commonly used numerical techniques and their computational abilities are discussed in Table 1, where one can see the advantages and disadvantages of using these numerical methods. For more details refer to Refs. 25 and 26.

DC TRANSFORMER DESIGN

Magnetic Circuits and Fields

Magnetic Circuit. The magnetic circuit is based on a dc electrical circuit analogy. Electromotive force, electric current, and resistance are replaced by magnetomotive force (mmf), magnetic flux, and magnetic reluctance respectively. The calculated results for reluctance and magnetic flux are reasonably accurate for geometries that exhibit a high degree of symmetry, for example a toroid. Unfortunately a simplified magnetic circuit cannot be used to represent complex geometric structures, such as a planar core or a matrix core. The only means to calculate accurately the magnetic quantities in this event is to solve Maxwell's equations with appropriate boundary conditions using a numerical technique.

Peak Flux Density. The peak flux density in ferrite cores must be limited so as to avoid magnetic saturation or to limit the temperature rise of the core due to increased core losses. Losses are the issue at high frequencies; and the use of a lower-loss core material or a reduction in the peak flux density may be necessary. Reducing the peak flux density necessitates an increase in the number of primary turns, and hence a smaller wire size for the same core-bobbin winding area.

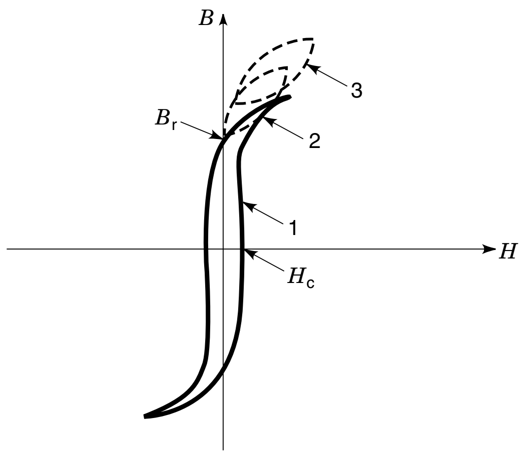

Figure 9. B–H curves for practical operation conditions: curve 1 for a transformer connected to a push–pull, half-bridge, or full-bridge converter, curve 2 for a flyback transformer operating in the discontinuous mode, curve 3 for a flyback transformer operating in the continuous mode.

With smaller wire size, primary and secondary currents are smaller and thus the available output power is decreased. The calculation of maximum transformer output power, peak flux density, core and bobbin areas, and coil current density can be found in a number of references (15,17,18).

Flux Distribution. The most desirable magnetic flux distribution is a uniform distribution. The distribution of magnetic flux within a core is influenced by the core geometry, the properties of the material, the location and geometry of the windings, and the operating frequency. Flux uniformity is more difficult to achieve at high frequencies because the flux tends to concentrate within a skin depth below the surface. Flux uniformity within the core can be obtained by choosing materials with a high resistivity and a low relative permeability. Unfortunately, low permeability means that some of the flux will exist outside of the core.

At very high frequencies the flux distribution will take on a standing wave pattern. This phenomenon is referred to as dimensional resonance and occurs when the wavelength is of the same order as the dimensions in a direction perpendicular to the magnetic field. The dimensional resonance frequency decreases as the core dimension increases or alternatively as the power rating of the device for a given frequency is increased. This problem can be avoided by reducing the size of the core, by choosing a material of lower relative permeability and permittivity, or by reducing the conductivity and the hysteresis loss of the material.

Practical Operating Conditions. The core of a transformer should never be operated close to saturation. Instead, minor loops such as the ones shown in Fig. 9 are traversed. Curve 1 represents the B–H curve for a transformer connected to a push–pull, half-bridge, or full-bridge converter. Curve 2 represents the B–H curve for a flyback transformer operating in the discontinuous mode. Curve 3 represents the B–H curve for a flyback transformer operating in the continuous mode (30).

In 20 kHz to 50 kHz PWM switching power supplies, the peak excursion of the flux density (B_m) is usually half of the saturation flux density (B_s). This results in a core loss of 2% of the rated input power, which is considered acceptable. For higher frequencies of operation, B_m is reduced further so as to keep the core losses at or below 2% of the rated input power. For unipolar flux applications, it is desirable to place a small air gap within the magnetic path of the core so as to maintain linearity at higher currents and to design for a higher flux swing in the presence of a dc mmf bias in the core.

Magnetic Core and Copper Losses

Magnetic Core Losses. Power losses in materials can be attributed to eddy currents, magnetic hysteresis, dielectric hysteresis, and gyromagnetic resonance absorbtion.

Eddy Current Losses. Eddy currents are lowered by using small magnetic particles separated from each other by a dielectric coating. This principle is applied in the manufacturing of powder iron cores. Further reductions in eddy currents are possible if the magnetic particles have low conductivity. This is the case for cores constructed from a ferrite material. The eddy current is given by the following expression:

$$P_e = k_e v f^2 (B_m) \tag{8}$$

where k_e is the eddy-current loss constant for the material, v is the volume of the core (m^3), f is the frequency of operation (Hz), and B_m is maximum flux density (T).

Hysteresis Losses. Magnetic or dielectric hysteresis depends on the shape of the crystals, the crystal material, the size of the crystal, and the stresses generated within the material and by the surrounding environment. Lower magnetic hysteresis can be achieved by using crystals whose size is smaller than the size of a single domain. Lower dielectric hysteresis is achieved by using a medium that has a low permittivity. Magnetic hysteresis loss is given by the following expression:

$$P_h = k_h v f (B_m^n) \tag{9}$$

where k_h is the hysteresis loss constant for a given material and excitation condition, v is the volume of the core (m^3), f is the frequency of operation (Hz), B_m is the maximum flux density (T), and n is a material-specific constant that ranges from 2 to 3. Dielectric losses are normally insignificant but contribute to the residual losses.

Gyromagnetic Resonance Losses. Gyromagnetic resonance occurs when the frequency of the source corresponds to the natural gyromagnetic resonant frequency of the material. Gyromagnetic resonance is avoided by selecting a frequency well below the gyromagnetic resonance frequency. The resonance frequency can be increased by decreasing the relative permeability of the magnetic material. Gyromagnetic resonance losses play a role at frequencies that are well beyond the region of interest.

Copper Losses (Skin and Proximity Effects). At high frequency, the major loss within windings is due to eddy currents produced by the skin and proximity effects. These effects can cause the winding losses to be significantly greater than the $I_{rms}^2 R$ loss calculated using the dc resistance of the winding (17).

The skin effect is caused by eddy currents induced in a wire by the magnetic field of the current carried by the wire itself. In contrast, the proximity effect is caused by eddy currents induced in a winding by magnetic fields of currents in adjacent windings either isolated from or directly connected to adjacent layers of the coil.

The calculation of the eddy current must be performed numerically and proceeds in the following fashion. From Maxwell's equations, we can derive a time-dependent magnetic vector potential equation

$$\nabla \cdot (\upsilon \nabla A) = -J_0(t) + J_e \tag{10}$$

where $\upsilon = 1/\mu$, J_0 is the current source, and J_e is the frequency-dependent eddy current defined as

$$J_e = \sigma \frac{\partial A}{\partial t} + \sigma \nabla \phi$$

Taking into consideration the quasistatic field ($j\omega \approx \partial/\partial t$) and neglecting the second term, one arrives at the following expression for the eddy current:

$$J_e = \sigma j\omega A \tag{11}$$

where σ is the conductivity and ω is the angular frequency. The amplitude of the eddy current is proportional to the operating frequency.

Skin Effect. The skin effect causes current in a wire to be confined to a thin skin on its outer periphery. The depth of this peripheral conducting area is inversely proportional to the square root of the frequency. As the frequency increases, a progressively larger part of the solid wire area is lost, thus increasing the ac resistance and ultimately the copper losses.

Currents in a dc transformer have square or quasisquare current waveforms that contain a sizable number of high-frequency Fourier components. The high skin resistance at these components makes the skin effect a concern even for a low-frequency converter. The majority of the energy in square current waveforms resides in the first three harmonics. The approximate skin depth for a given harmonic component can be calculated using the following expression:

$$\delta = \sqrt{\frac{2}{\omega\mu\sigma}} \tag{12}$$

where $f = \omega/2\pi$ is the frequency of the applied magnetic field, μ is the magnetic permeability of the core material, and σ is the conductivity of the magnetic material.

Proximity Effect. The induced eddy currents due to the proximity effect can be many times greater in amplitude than the net current flowing in an individual winding. Higher copper losses can be generated by the proximity effect than by the skin effect, especially in multilayer windings. Mathematical expressions for the ac/dc resistance ratio and its analysis are given in detail in a number of papers, notably the ones by Dowell (31) and Perry (32).

Design Rules of Thumb

At high frequencies it is common to use litz wire or foil wire. The following rules of thumb for reducing eddy current losses apply: litz wire is more effective for nearly sinusoidal currents; counterflowing currents should be arranged to flow on facing conductors whenever possible; leads and extraneous conductors should be minimized in high-flux regions; full winding layers should be used; the primary and secondary windings should be interleaved, and the number of winding portions maximized; two windings in parallel, with the same number of turns and with one winding optimized for ac losses and the other winding optimized for dc losses, should be used for dc inductors; the layer thickness should be optimized, and the optimum is a function of the skin depth, the number of layers, the magnetic field at the conductor's surface, and the harmonic content; sprial windings should have a winding width that is proportional to the radius; the layer–layer spacing should be minimized to minimize the total entrant flux; the turn–turn spacing should be maximized to minimize the entrant flux density; thick multiturn single-layer windings should be avoided so as to minimize conductor edge eddy currents (32–34).

INTRA- AND INTERWINDING CAPACITANCE AND HIGH-VOLTAGE CONSIDERATIONS

Intra- and Interwinding Capacitance

Intra- and interwinding capacitances are parasitic elements associated with any transformer. Inductors include only interwinding capacitances. These capacitances can be exploited in a circuit context or can contribute to undesirable high-frequency transients. In the latter case, the distributed primary and secondary shunt capacitances in transforms (intrawinding capacitances) in conjunction with the transformer leakage inductances will generate resonance behavior each time the primary or secondary winding is subjected to a switching transient.

A significant path for unwanted noise currents is through the intewinding capacitance of the output transformer. This capacitance couples high-frequency voltage harmonics directly from one winding to the other.

A simple means of estimating intra- and interwinding capacitances has been described by Snelling (35). As a general rule, leakage inductances and interwinding capacitances both tend to decrease as the voltage rating of the transformer increases. The power rating and operating frequency will also influence these parameters.

High-Voltage Considerations

Some applications require a high-voltage dc output or source. High output voltages can be obtained using a flyback converter, or a resonant converter and transformer followed by a full-wave diode bridge or a voltage multiplier circuit. At higher voltages it may be necessary to have multiple secondary windings and rectifiers. The application requirements will dictate the choice of high-voltage dc transformer circuit topology.

Dielectric losses can become an issue in high-voltage high-frequency transformers, specifically in regions where the electric field intensity is high. In many cases the geometry of the core, the winding layout and shape, and the core material must be chosen carefully so as to minimize the difference between the peak and the mean electric field intensity within the core material. Also, insulation grading, electric field grading, and minimum interwinding spacing must be chosen so as to prevent the initiation of corona discharges. In some cases it may also be necessary to include overvoltage protection devices (36,37).

EFFICIENCY, POWER DENSITY, AND THERMAL ANALYSIS

Efficiency

For a given power throughput, the core loss increases as the core size and flux density swing increase, and the copper loss increases as the core size and flux density swing decrease. These two requirements are in conflict, and a compromise selection is made. Optimum efficiency need not occur when core and copper losses are equal. The precise loss apportionment for maximum efficiency depends on the core material, core geometry, and operating frequency.

Power Density

By increasing the frequency, the size of the transformer can be reduced and the power density of the transformer will be increased. This is at the expense of an increase in the temperature of the core, whose magnitude depends on the total internal core loss, the core surface area, the thermal conductivity of the core, and the external radiative and convective heat transfer coefficients. Most dc transformers are cooled by means of natural convection, in which case the heat transfer coefficient is poor. The size of high-power-density transformers is too small to allow for enough surface area from which the heat can radiate or convect. This limit on heat transfer rate ultimately enforces an upper limit on the power density (38). Aside from the use of lower-loss materials, improved heat transfer properties can be obtained by using one or more of the following structures: attached heat sinks, planar core structures, external metallic EMI shields, and shielded windings.

Thermal Analysis

Simple one-dimensional models for heat transfer are used currently to estimate the temperature rise in the core. Dc circuit models analogous to electric circuit models are used to calculate the temperature drops within a medium. Current sources are replaced by power sinks, voltage differences by temperature differences, and electrical resistances by thermal resistances (16). A more accurate analysis can be obtained using the numerical techniques and appropriate boundary conditions as mentioned in the above section.

BIBLIOGRAPHY

1. S. Cuk, Basics of switched-mode power conversion: Topologies, magnetics, and control, Power Conversion International, in B. K. Bose (ed.), *Modern Power Electronics, Evolution, Technology, and Applications,* Piscataway, NJ: IEEE Press, 1992, pp. 265–296.
2. T. Zaitsu, O. Ohnishi, and T. Inoue, Piezoelectric transformer operation in thickness extensional vibration and its application to switching converter, *IEEE PESC'94,* 1994, Vol. I, pp. 585–590.
3. B. K. Bose, *Microcomputer Control of Power Electronics and Drives,* Piscataway, NJ: IEEE Press, 1987.
4. B. K. Bose, Modern power electronics, evolution, technology, and applications, in B. K. Bose (ed.), *Modern Power Electronics, Evolution, Technology, and Applications,* Piscataway, NJ: IEEE Press, 1992.
5. C. H. Ahn and M. G. Allen, A new toroidal-meander type integrated inductor with a multilevel meander magnetic core, *IEEE Trans. Magn.,* **30** (1): 73–79, 1994.
6. J. Lu, F. P. Dawson, and S. Yamada, Analysis of planar sandwich transformer for high frequency switching converters, *IEEE Trans. Magn.,* **31** (6): 4235–4237, 1995.
7. H. Tsujimoto and O. Ieyasu, High frequency transmission characteristic of C0-planar film transformer fabricated on flexible polyamide film, *IEEE Trans. Magn.,* **31** (6): 4233–4234, 1995.
8. F. Wong et al., Application of high frequency magnetic components for switching resonant mode power supply, *IEEE Int. Conf. Ind. Technol., ICIT'96,* 1996, pp. 406–410.
9. D. Kuhn, E. Lo, and T. Robbins, Powering issues in an optical fiber customer access network, *Proc. IEEE INTELEC'91,* 1991, pp. 51–58.
10. W. J. Mcnut, T. J. Blaock, and R. A. Hinton, Response of transformer windings to system transient voltages, *IEEE Trans. Power Appar. Syst.,* **93** (2): 457–467, 1974.
11. C. A. Rosen, Ceramic transformers and filters, *Proc. Electron. Component Symp.,* 1956, p. 205.
12. T. Zaitsu et al., 2 MHz power converter with piezoelectric ceramic transformer, *IEEE Intelec. Proc.,* 1992, pp. 430–437.
13. T. Zaitsu, O. Ohnishi, and T. Inoue, Piezoelectric transformer operation in thickness extensional vibration and its application to switching converter, *IEEE PESC'94,* 1994, Vol. I, pp. 585–590.
14. C. Y. Lin and F. C. Lee, Design of piezoelectric transformer converter and its matching network, *IEEE PESC'94,* 1994, Vol. I, pp. 607–612.
15. N. Mohan, T. M. Undeland, and W. P. Robbins, *Power Electronics: Converters, Applications, and Design,* 2nd ed., New York: Wiley, 1995.
16. K. Billinges, *Switch Mode Power Supply Handbook,* New York: McGraw-Hill, 1989.
17. A. I. Pressman, *Switching Power Supply Design,* New York: McGraw-Hill, 1991.
18. S. S. Ang, *Power Switching Converters,* New York: Dekker, 1995.
19. E. R. Hnatek, *Design of Solid State Power Supplies,* 3rd ed., New York: Van Nostrand Reinhold, 1989.
20. B. Carsten, Design techniques for transformer active reset circuits at high frequencies and power levels, *Proc. HFPC,* 1990, pp. 235–246.
21. B. Andreycak, Active clamp and reset technique enhances forward converter performance, *Unitrode Power Supply Design Seminar,* 1994, SEM-100, pp. 3.1–3.18.
22. Q. Chen, F. C. Lee, and M. Jovanovic, Small-signal analysis and design of weighted voltage control for a multiple-output forward converter, *IEEE Trans. Power Electron.,* **10** (5): 589–596, 1995.
23. G. K. Schoneman and D. M. Mitchell, Closed-loop performance comparisons of switching regulators with current-injected control, *IEEE PESC-ESA Proc.,* 1985, pp. 225–233.
24. F. C. Lee and R. A. Carter, Investigations of stability and dynamic performances of switching regulators employing current-injected control, *IEEE PESC Rec.,* 1981, pp. 3–16.
25. J. Sabonnadier and A. Konrad, Computer EM fields, *IEEE Spectrum,* pp. 52–56, 1992.
26. M. N. O. Sadiku, *Numerical Techniques in Electromagnetics,* Boca Raton, FL: CRC Press, 1994.
27. J. K. Sykulski, *Computational Magnetics,* London: Chapman & Hall, 1995.
28. S. R. H. Hoole, *Computer-Aided Analysis and Design of Electromagnetic Devices,* Amsterdam: Elsevier, 1989.
29. K. Yamaguchi and S. Ohnuma, Characteristics of a thin film microtransformer with circular spiral coils, *IEEE Trans. Magn.,* **29** (5): 2232–2237, 1993.

30. M. Brown, *Power Supply Cookbook,* Newton, MA: Motorola, Butterworth-Heinemann, 1994.
31. P. L. Dowell, Effects of eddy current in transformer windings, *Proc. IEEE,* **113** (8): 1387–1394, 1966.
32. M. Perry, Multiple layer series connected winding design for minimum losses, *IEEE Trans. Power Appar. Syst.,* **PAS-98** (1): 116–123, 1979.
33. N. Dai and F. C. Lee, Edge effect analysis in a high-frequency transformer, *IEEE PESC'94,* 1994, Vol. II, pp. 850–855.
34. J. Lu, S. Yamada, and H. B. Harrison, Application of HBFEM in the design of switching power supplies, *IEEE Trans. Power Electron.,* **11** (2): 347–355, 1996.
35. E. C. Snelling, *Soft Ferrites—Properties and Applications,* London: Butterworth, 1988.
36. R. D. Middlebrook, Input filter considerations in design and application of switching regulators, *IEEE PESC Rec.,* 1977, pp. 36–57.
37. D. M. Mitchell, Damped EMI filters for switching regulators, *IEEE Trans. Electromagn. Compat.,* **EMC-20** (3): 457–459, 1978.
38. R. Farrington, M. M. Jovanovic, and F. C. Lee, Design oriented analysis of reactive power in resonant converters, *IEEE Trans. Power Electron.,* **8** (4): 411–422, 1993.

JUN W. LU
Griffith University

FRANCIS P. DAWSON
The University of Toronto

SOTOSHI YAMADA
Kanazawa University

TORU HIGASHI
Kumamoto University

ICHIRO SASADA
Kyushu University

MASAHIRO YAMAGUCHI
Tohoku University